

## Evaluation of steel fiber distribution in concrete by computer aided image analysis

Josef Fládr<sup>a</sup>, Petr Bílý\* and Iva Broukalová<sup>c</sup>

Department of Concrete and Masonry Structures, Faculty of Civil Engineering, Czech Technical University in Prague, Thákurova 7, 16629 Prague, Czech Republic

(Received May 21, 2019, Revised June 10, 2019, Accepted June 11, 2019)

**Abstract.** Several methods for evaluation of uniformity of distribution of fibers in steel-fiber-reinforced concrete (SFRC) exist today. All of them are either ineffective, biased or their execution requires special expensive equipment. A promising new approach based on computer aided SFRC digital image analysis was developed and tested with excellent results. The process of taking and adjusting the pictures of SFRC samples is described in the paper. ASEF (Automatic Specimen Evaluation of Fibers) program was prepared in MATLAB environment for quick and accurate detection of fibers in the photographs. Basically, the detection algorithm exploits different reflectance of steel fibers and concrete matrix. No unusual devices are needed for employment of the method. The whole procedure is very simple and can be used successfully in both laboratory and construction site. Examples of application of the method are presented in the paper. Several mixtures of high-performance concrete containing 120 kg of steel fibers per cubic meter of concrete were compared with respect to the uniformity of dispersion of fibers, optimal mix composition was selected. Large scale specimens made of normal strength SFRC for tunnel linings were examined, the analysis led to a conclusion that sufficient uniformity of dispersion of the fibers in the mix was reached.

**Keywords:** fiber-reinforced concrete; distribution of fibers; homogeneity; computer aided design; digital image analysis; MATLAB

### 1. Introduction

In the last five decades, there have been conducted many research programs devoted to the use of steel fibers and properties of steel-fiber-reinforced concrete (SFRC). In the recent years, SFRC is becoming more and more common in civil engineering applications due to many reasons. The fibers positively affect mechanical properties, mainly flexural and shear resistance of SFRC members (Spinella 2013, Hwang *et al.* 2015). Fibers improve durability of cementitious composites to freeze-thaw cycling, deicing agents or chemical attack, therefore steel and polymer fiber reinforced concretes are used in transport infrastructure structures (Bílý *et al.* 2015, Fládr *et al.* 2016). At the basis of the durability lies the intrinsic crack control of SFRC, whereby ingress of deleterious liquids and gases is deterred (van Zijl *et al.* 2012). Both steel and polymer fibers are used to improve characteristics of concretes containing waste aggregate (Katzner and Domski 2013,

---

\*Corresponding author, Professor, E-mail: petr.bily@fsv.cvut.cz

<sup>a</sup> Ph.D., E-mail: josef.fladr@fsv.cvut.cz

<sup>b</sup> Associate Professor, E-mail: iva.broukalova@fsv.cvut.cz

Sebaibi *et al.* 2014). In connection with current global security threats, many researchers engage themselves with the topic of performance of SFRC exposed to blast or impact loads (Perumal 2014, Foglar 2015, 2017). Excellent results have been reported, mainly thanks to the outstanding ductility of the material.

Mechanical properties and geometry of the fibers are very important to ensure the best possible function of dispersed reinforcement in concrete. Over 90 % of currently produced steel fibers are engineered (shaped) fibers with the shape adjusted to maximize the anchorage of fibers in concrete. Likewise, more than 90 % of fibers exceed the tensile strength of 1000 MPa (Katzner and Domski 2012).

Advantages of SFRC containing the high-quality steel fibers can be fully exploited only in case that the material is homogeneous in the whole volume of a structural element. Achieving even distribution of fibers in concrete matrix is a demanding task from the technological point of view. It is well known that in theoretical case of pure bending, alignment of fibers in one direction is desirable (Kang *et al.* 2008). However, as most structural members are loaded by combination of bending, shear and compression, even alignment of fibers in all three directions is usually more favorable. The tensile properties of fiber-reinforced concrete are governed mainly by the number, dispersion and orientation of fibers in the cracking area.

The position of reinforcing bars in reinforced concrete can be controlled visually before concreting. Such a simple control is not possible in case of fibers dispersed in SFRC. Verification of uniformity of distribution of the fibers in hardened material is one of the most important, but also most difficult parts of SFRC design and production process. Therefore accessible and reliable testing methods are needed. Various currently available methods will be briefly described in the next chapter. A new approach developed by the authors will be detailed in the rest of the paper.

## 2. Current methods for evaluation of distribution of fibers in SFRC

The easiest way to qualitatively assess the uniformity of dispersion of fibers in concrete is “visual control” performed by experienced specialists. The samples are cut by a saw and examined by responsible people – concrete production plant representative, investor representative, engineering supervision etc. Completely inappropriate concrete mixes containing bundles of fibers can be eliminated, but the evaluation is very subjective, not allowing quantitative comparison of different concrete mixes.

The coordinates of individual fibers in SFRC cross-section may be measured manually and then evaluated mathematically. So called “manual evaluation method” or “counting method” gives precise information about distribution of fibers in the section, however the execution is very fatiguing and ineffective in terms of time. It is still used by some researchers (Pereira de Oliveira *et al.* 2013), but it is unsuitable for practical use in larger scale.

Another approach, so called “crushing method”, is based on extraction of fibers from crushed samples. SFRC samples are crushed, fibers in different samples are counted or weighed and the results are compared. Thus information about concentration of fibers in samples taken from different parts of a larger element can be obtained. Crushing can be performed by hammer or by compression machine (Ferrara and Meda 2006). Fibers can be picked manually or more efficiently by magnetic separation (Ferrara *et al.* 2012). In any case, the method is laborious and provides just very rough opinion on the distribution of the fibers in the investigated element.

Thanks to electric conductivity of steel fibers, “inductive methods” can be used for non-destructive testing of fiber distribution (figure 1a; Torrents *et al.* 2012, Vitek *et al.* 2013). The



(a) SFRC sample in the coil (reprinted from Vitek *et al.* 2013)



(b) Depth magnetic probe in SFRC sample

Fig. 1 Inductive methods

equipment is composed of impedance analyzer and a coil that receives electric current and generates magnetic field. When SFRC sample is placed inside the coil, modification of magnetic permeability of the medium takes place based on the amount of fibers in the sample. This modification leads to a change in the inductance measured with the impedance analyzer. According to the established test procedure, the measurement is performed in three directions perpendicular to the faces of the specimen. Thus amounts of fibers orientated in particular directions of the sample may be estimated. The problem is that the measurement only gives average values without providing any information on the scatter or distribution of the fibers.

A modification of the previous method was proposed by Vodička *et al.* (2013, 2016). Instead of placing the sample inside the coil, the authors developed a depth probe that can be inserted into a borehole in SFRC specimen (figure 1b). The advantage is that this method is not limited by the size of the sample and it can be used also for large scale elements. However, the user still obtains just rough information about the amount of fibers in the selected area of the element.

Probably the most sophisticated method used for evaluation of distribution of fibers is “X-ray computed tomography” (CT). SFRC sample is placed inside CT scanner, 3D map of fibers inside the sample is created and digitally processed to obtain fiber distribution characteristics (figure 2; Eik *et al.* 2013). CT technology allows comprehensive assessment of distribution of not only the fibers, but also porosity characteristics of concrete specimens. On the other hand, CT scanners are complex and expensive devices that are usually not available to concrete researchers, let alone the designers of concrete structures and concrete producers. Furthermore, image processing is quite demanding and advanced knowledge of programming and graphical software tools is required (Ponikiewski *et al.* 2015). Therefore this method is applicable only for cutting-edge research, not for everyday use in the construction industry.

All the methods mentioned above suffer from certain disadvantages. Visual control is biased, counting method is time consuming, crushing method is laborious and inaccurate. Inductive methods do not give the full picture of distribution of fibers in the cross-section. CT requires the use of special devices which are usually not at disposal of concrete researchers or concrete production companies. Therefore, none of the methods is able to satisfy the fundamental requirements for wide use – to provide exact results at low costs and in reasonable time.

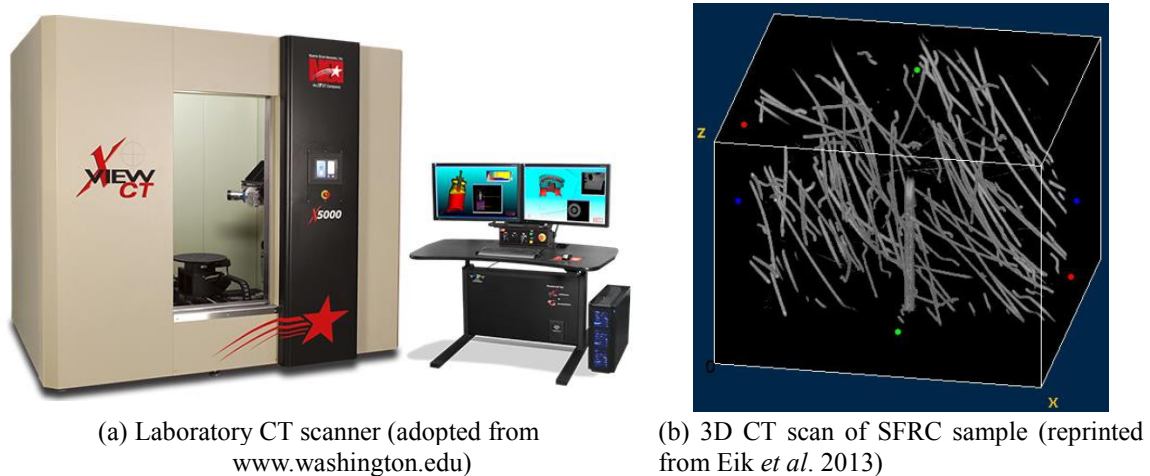


Fig. 2 X-ray computed tomography (CT)

According to the opinion of the authors, the method that best meets all the above mentioned needs is 2D digital image analysis. Ordinary photograph of a section of a concrete sample is taken, coordinates of fibers are determined using a software tool and uniformity of dispersion of fibers is appraised. Several authors have applied this method before with good results (Burcu and Tasdemir 2012, Sebaibi *et al.* 2014). However, they used complicated software for treatment of the images and they did not explain the process of acquiring the photographs which is crucial for accurate results. Therefore the authors decided to develop a user-friendly software tool to enable wider use of computer aided SFRC digital image analysis and to provide guidelines for taking and processing of the images.

### 3. Computer aided SFRC digital image analysis

#### 3.1 The basic idea of the method

The method is based on computer aided analysis of digital image of a section of SFRC sample. The difference in reflectance of shiny steel fibers and dull concrete matrix is exploited. If the light shines at a suitable angle, the section planes of freshly cut fibers reflect the rays of light. The photograph of the surface is taken and analyzed by ASEF software utility that detects particular fibers. The stronger is the contrast between the fibers and the matrix, the higher is the probability of correct detection of the fibers in the section.

As will be explained further, the execution of the method is fast and simple, it does not require any unusual devices and it gives accurate and unbiased results. The results are not dependent on subjective attitude of the person performing the analysis. The method can be applied in both laboratory and construction site. To take the image of SFRC sample, just a suitable camera, stand, one-colored textile, length scale and light source are needed.

#### 3.2 Photographing

Taking a photograph is the key part of the whole process. A camera having adequate resolution (at least 8 Mpx according to authors' experience) should be used. Higher resolution of the camera

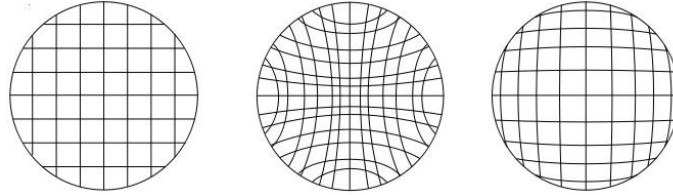


Fig. 3 Undistorted grid (left), pincushion distortion (middle), barrel distortion (right)

decreases the risk of formation of problematic image pixels – pixels where the evaluation algorithm of the program could encounter problems when deciding if the pixels represent a fiber or an aggregate grain.

Distortion of the picture (barrel or pincushion, see figure 3) must be avoided. To obtain absolutely perfect photo, a professional camera with fixed lens and medium focal length should be used. In practice, it is possible to use standard camera with zoom lens if the photo is taken from sufficient distance from the object and the distortion is not visible by naked eye. The distortion leads to misrepresentation of the results as the program is not able to determine the total cross-sectional area of the sample and positions of the fibers correctly.

Setup of white balance of the camera is very important as well. In photography, white balance is an operation consisting in color compensation of the object (and its lighting conditions) that is performed to make the color rendition of the image as close as possible to the perception of the human eye. While taking the pictures at standard lighting conditions, automatic white balance is acceptable. In case of artificial lighting or if the pictures are taken with the use of flashlights, manual setup is preferred as automatic white balance could suppress the color differences between the fibers and the matrix which are crucial for correct evaluation of the image.

Background of the object must be selected carefully. One-colored dull background is preferred. The authors recommend a dull black textile.

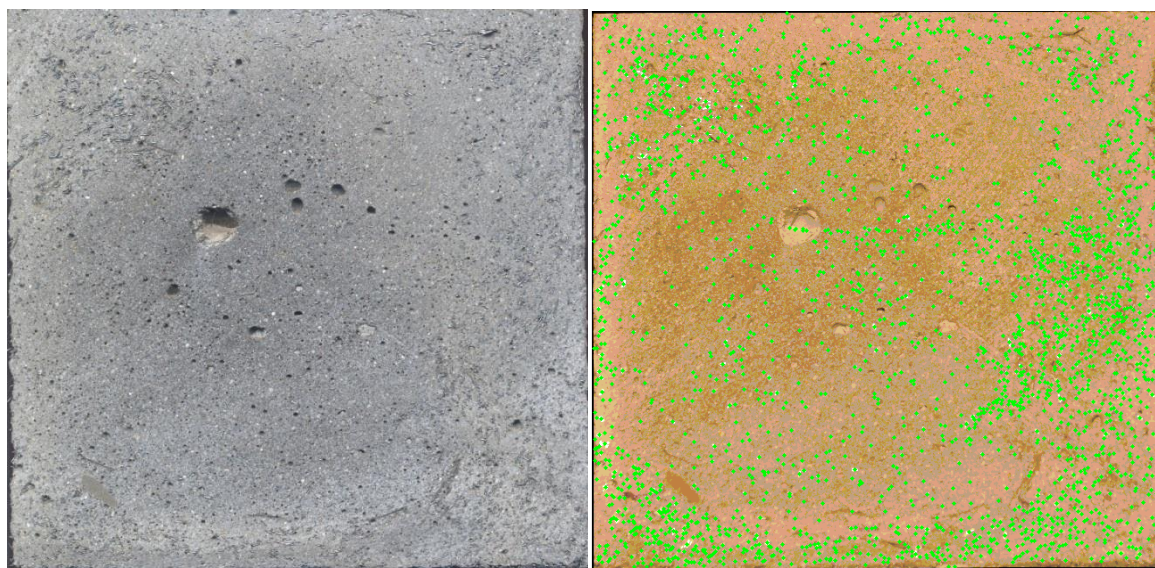
Correct lighting of the sample is essential. The lights must be fixed in the position which causes the most significant reflection of light from the cut planes of the fibers. A stand should be used to secure the location of the lights. It is not necessary to use expensive flashlights to illuminate the sample, an ordinary halogen lamp from the construction site will work just fine.

As was said earlier, the method works with sections of SFRC specimens. Cutting is performed by concrete saws equipped with water cooling system, therefore the surface of the sample is moistened during the process. The surface mustn't be covered by water film during photographing as the reflectance of concrete matrix would be increased and the contrast between the steel fibers and the matrix would be reduced. The surface should be dried by absorbent fabric. The photo should be taken as soon as possible after the cutting to avoid corrosion of the fibers.

Alternatively, suitable images can be also obtained by scanning the specimens in an ordinary flatbed office scanner. One just has to keep in mind that the scanner glass might be scored by steel fibers extending from the surface of SFRC sample.

### 3.3 Image adjustment

Prior to evaluation, the margins of the pictures should be cut in an arbitrary image processing software (figure 4a). Real dimensions of the area of the sample depicted on the photo should be determined. This can be done the most easily by placing a length scale next to the sample while taking the photo.



(a) Original photo of section of SFRC specimen

(b) Positions of the fibers detected by ASEF software. The contrast and color saturation of the image were adjusted in graphic software with the aim to facilitate detection of fibers.

Fig. 4 Section of SFRC specimen

Additional processing of the image is suitable (but not necessary) to distinguish the fibers from the matrix more significantly (figure 4b). Any available graphic software can be used, including very simple freeware programs such as IrfanView. Usually it is beneficial to increase the contrast of the picture, slightly increase the color saturation and to perform the gamma correction. Sharpening of the image should be avoided as it leads to creation of new bright areas in the image that can be misinterpreted as fibers.

### 3.4 Image evaluation

Evaluation is the simplest part of the method as it is done with the use of user-friendly software ASEF (Automatic Specimen Evaluation of Fibers) that was developed by the authors for this purpose. ASEF was created in MATLAB programming language, but it is not necessary to own MATLAB license to run the program. Installation of free MATLAB Compiler Runtime (MCR) library will do.

The principle of the program can be described as follows. In the first step, image of the sample in jpg or png format is loaded. Dimensions of the image  $d_x$ ,  $d_y$  [mm] and cross-sectional area of one fiber  $a_f$  [mm<sup>2</sup>] are entered (figure 6, upper left window). In the image, the color representing the fibers must be selected by the user with the cursor. The selected color is saved as a vector of RGB (red – green – blue) color space coordinates:

$$\vec{c}_{sel} = (r_{sel}, g_{sel}, b_{sel}) \quad (1)$$

Then the detection algorithm is run to look up the fibers. Each pixel of the image is characterized by its own RGB color space coordinates:

$$\vec{c}_{ij} = (r_{ij}, g_{ij}, b_{ij}) \quad (2)$$

Sizes of RGB color vector of the selected color  $s_{sel}$  and RGB color vectors of individual pixels  $s_{ij}$  are calculated according to formulae:

$$s_{sel} = |\vec{c}_{sel}| = \sqrt{r_{sel}^2 + g_{sel}^2 + b_{sel}^2} \quad (3)$$

$$s_{ij} = |\vec{c}_{ij}| = \sqrt{r_{ij}^2 + g_{ij}^2 + b_{ij}^2} \quad (4)$$

A pixel is evaluated as a potential fiber in case that:

$$s_{ij} \geq F \cdot s_{sel} \quad \wedge \quad r_{ij} \geq F \cdot 215 \quad (5)$$

where  $F$  is a sensitivity factor. The second part of the condition says that the red RGB coordinate of the pixel must be more than or equal to 215. Based on the long term experience of the authors, fibers in correctly taken image are seldom represented by a shade of gray having red coordinate less than 215.

The user can change the sensitivity of the detection algorithm manually if he is not satisfied with the detection of the fibers, for example if the program determines some aggregate grains as fibers by mistake or if it does not find any of the fibers. This can be done by the horizontal scroll bar in the upper right window of the program in figure 6. The scroll bar changes the sensitivity factor  $F$ .

Of course not all the pixels identified as potential fibers can be counted as fibers. There are two main aspects that must be taken into account. Firstly, each fiber in the image consists of several pixels meeting the pair of conditions (5), but only one of the pixels can be counted as fiber in the analysis. Considering the cross-sectional area of one fiber  $a_f$  and circular shape of the cross-section, the theoretical radius of the fiber is  $r$  and minimum distance between the centroids of two fibers is:

$$l_{min} = 2r = 2\sqrt{\frac{a_f}{\pi}} \quad (6)$$

Secondly, the fibers cut askew could be incorrectly identified as multiple fibers. Therefore, if the program finds two (or more) centroids whose distance is equal to  $l_{min}$ , they are treated as one fiber and just the centroid of the whole fiber is used for further analysis.

Special subroutines are incorporated in ASEF to take into account the above mentioned aspects. The pixels identified as centroids of the fibers are marked with colored dot (figure 5 and figure 6, upper right window), coordinates of fibers are determined and the results are prepared in both graphical (figure 6, lower window) and numerical form (exportable data sets).

The analysis results in two plots. The first one is a frequency histogram showing groups of fibers with given maximum distance from the closest fiber (figure 6, lower left window). For the entirely homogeneous material, the distances between all the fibers should be the same, resulting in just one column in the histogram. In practice, material with less than 5 dominant neighboring columns can be considered homogeneous, the other columns should be insignificant.

The main output is the curve comparing the real distribution of the fibers in the cross-section with the ideal one (figure 6, lower right window). This is a summation curve showing the dependence of the relative number of fibers on the relative distance from the bottom edge of the



Fig. 5 Detail showing one part of analyzed SFRC cross-section. Fibers highlighted by yellow ellipses are the fibers that were cut askew (i.e. the cut plane was not perpendicular to the longitudinal axis of the fiber). Special inbuilt subroutine of ASEF guarantees that the whole cross-section will be treated as one fiber

sample. In ideal case of absolutely uniform distribution of fibers, the dependence should be linear with 1:1 slope. The closer is the real curve to that line, the more uniform is the dispersion of the fibers in SFRC.

For quick evaluation of uniformity, proportional deviation between the real and the ideal curve is calculated under the plot. The number is obtained as an average of deviations in particular points of the curve according to formula

$$\Delta = \frac{1}{n} \sum_{i=1}^n |k_i - j_i| \quad (7)$$

where  $n$  is the number of points of the real curve,  $k_i$  is the relative amount of fibers in the given point of the real curve and  $j_i$  is the relative amount of fibers in the given point of the ideal curve.

ASEF also calculates the reinforcement ratio of the cross-section as ( $n$  is the number of fibers looked up in the analyzed cross-section):

$$\rho = \frac{n \cdot a_f}{d_x \cdot d_y} \quad (8)$$

ASEF performs the detection of fibers automatically in the first step. If the user is not satisfied with the quality of the detection of fibers, the sensitivity of the detection algorithm can be adjusted manually. The program will perform a new analysis and compare it to the original one. In figure 6 (lower right window), the automatically determined fiber distribution curve is depicted in green, the curve after manual adjustment in blue, the ideal curve is red.

The user can export coordinates of the fibers, points of the curves and histograms in xls format for further processing. Images of SFRC section and plots can be stored in jpg format.

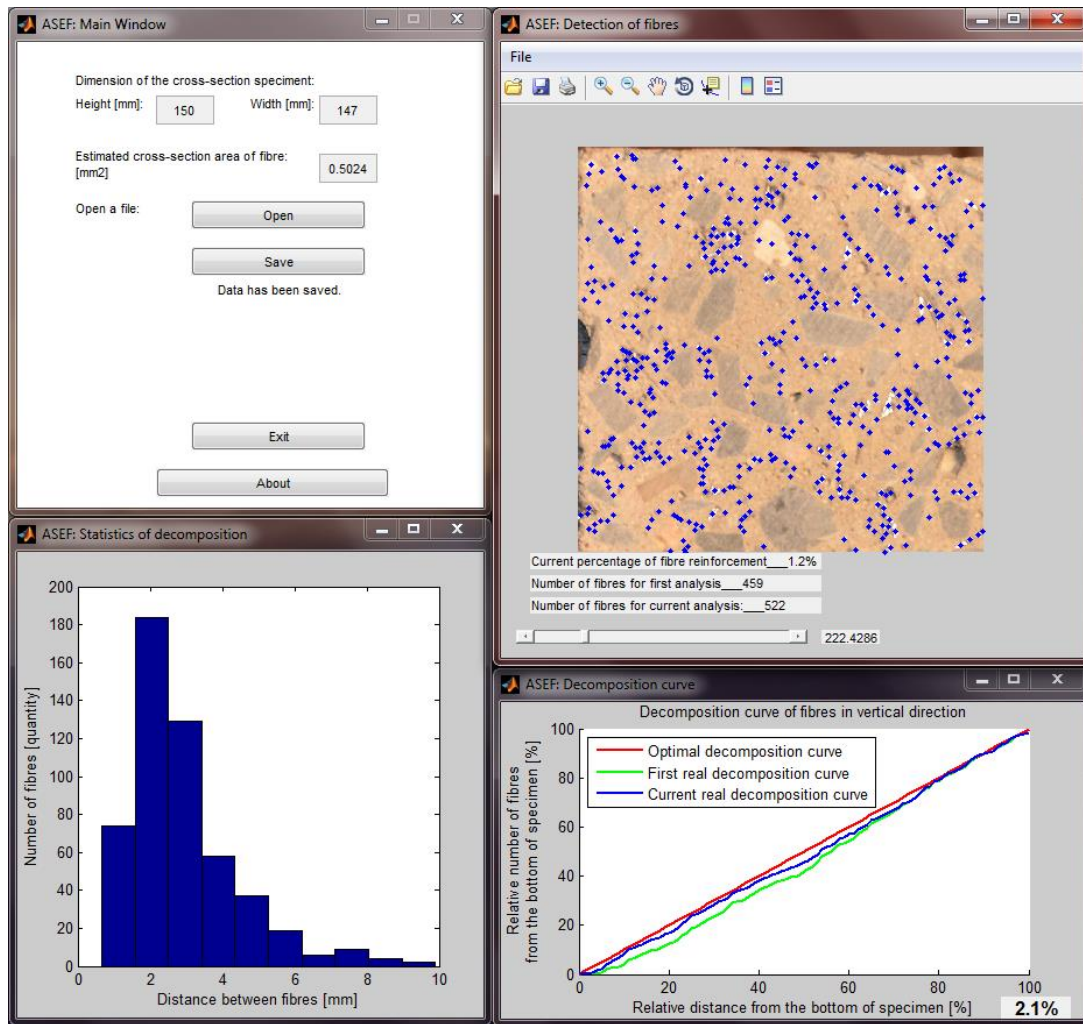


Fig. 6 Image analysis in ASEF software

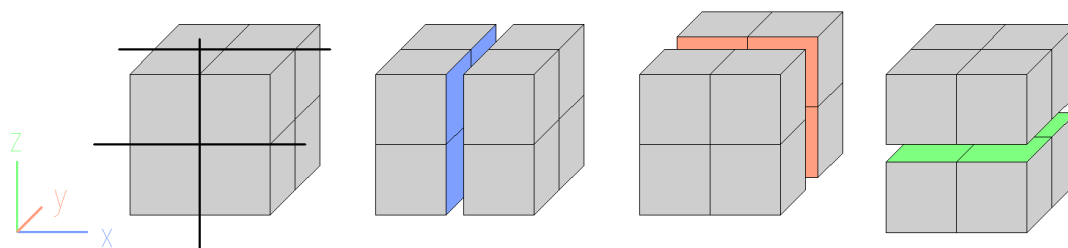


Fig. 7 Cutting of cube specimen appointed for 3D fiber dispersion analysis

### 3.5 3D fiber dispersion analysis

ASEF software is primarily designed for processing of 2D digital images of SFRC sample sections. If a 3D analysis of distribution of fibers in the specimen is to be performed, the sample

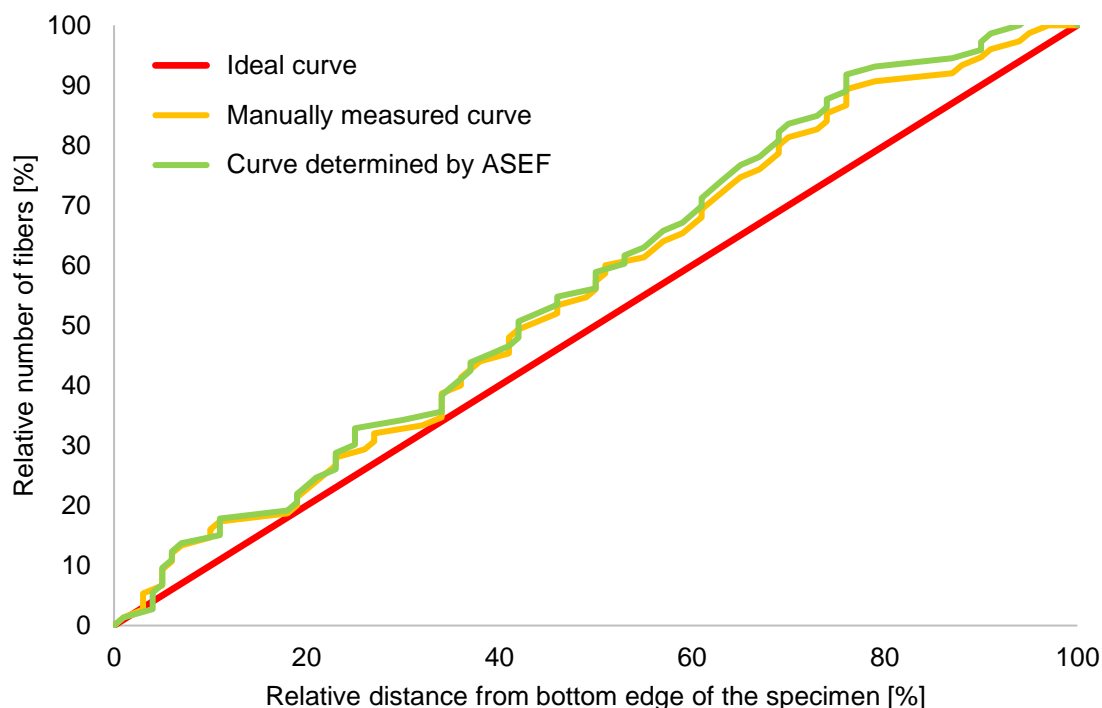


Fig. 8 Comparison of fiber distribution determined manually and by ASEF software

Table 1 Composition of the mixtures

Label	Cement [kg/m <sup>3</sup> ]	Water [kg/m <sup>3</sup> ]	Aggregate size [mm]	Aggregate [kg/m <sup>3</sup> ]	Steel fibers [kg/m <sup>3</sup> ]
D1	500	202	0/4+4/8	874+700	120
D2	500	202	0/4	1442	120
D3	600	228	0/2	1308	120
D4	800	240	0/1	1041	120

has to be cut in more parts and each section has to be evaluated separately. Then the distribution of fibers in particular sections and/or directions can be assessed.

#### 4. Verification of reliability of ASEF software

The first verification of evaluation function of ASEF program was performed on a series of 150 mm cube samples made from SFRC containing 30 kg of steel fibers per 1 m<sup>3</sup> of concrete. The low fiber content was selected because the verification was performed by straightforward counting method based on manual measurement of positions of all the fibers in the section. The comparison for one of the samples is presented in figure 8. The agreement between the two methods was excellent.

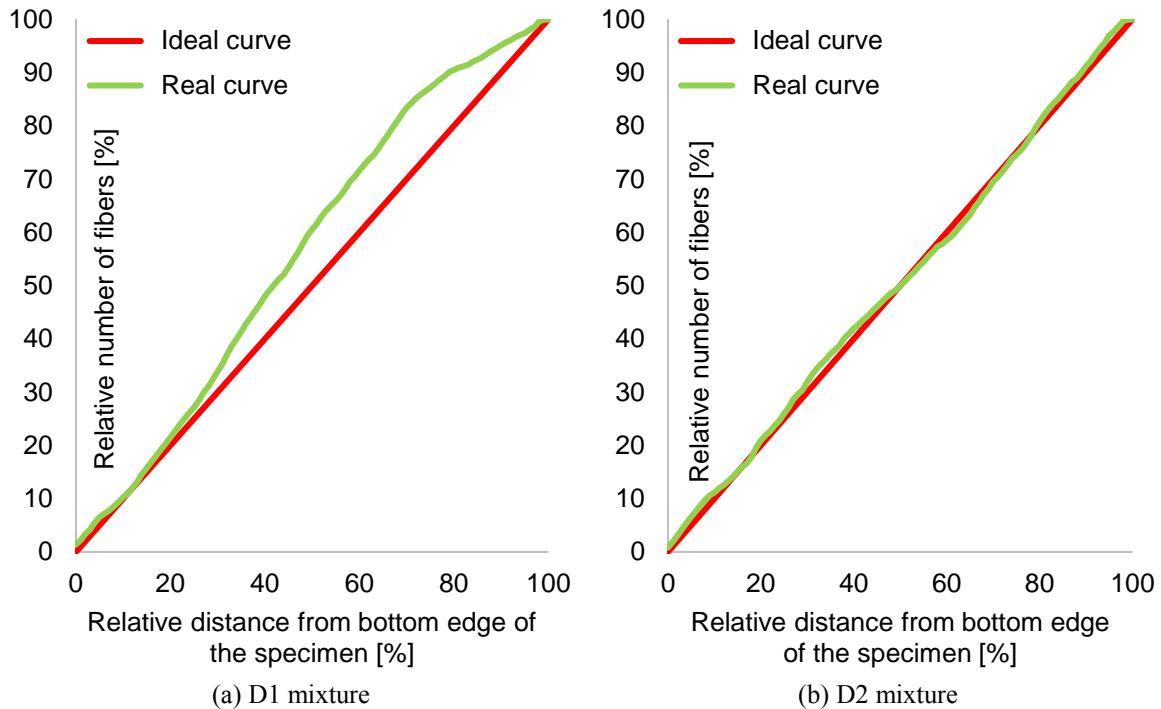


Fig. 9 Distribution of fibers in D1 and D2 mixtures

## 5. Examples of application of the method

### 5.1 High-performance concrete (HPC) mix design optimization

Digital image analysis method described above was exploited for determination of influence of aggregate grain size on the uniformity of distribution of fibers in SFRC with high content of steel fibers. For this purpose, three 150 mm cube samples were produced for each of the four mixtures described in table 1. SFRC contained  $120 \text{ kg/m}^3$  of steel fibers. Such high fiber content is not used very often, but in case of special concretes such as ultra-high performance concretes (UHPC), similar dosages may be used in some cases (Hadl *et al.* 2015, Vaitkevičius *et al.* 2016, Ma *et al.* 2016).

The same steel fibers were dispersed in all the mixtures. The parameters of the fibers were 13 mm length, 0.2 mm diameter, 2750 MPa tensile strength of steel. These fibers were selected due to their compatibility with the aggregate used. If longer fibers were used, segregation of fibers and aggregates would probably occur in case of D4 mixture where 0/1 aggregates were employed.

During production of the specimens, the same technological approach was followed for all the samples. The main concern was the same compaction time of all the samples. After hardening phase, all the specimens were divided by two sections into three 150x150x50 mm bodies. The cutting was done parallel to the direction in which the material was compacted. After that, the sections were analyzed by ASEF program. The resulting curves describing the distribution of fibers in the section are presented in figures 9 and 10.

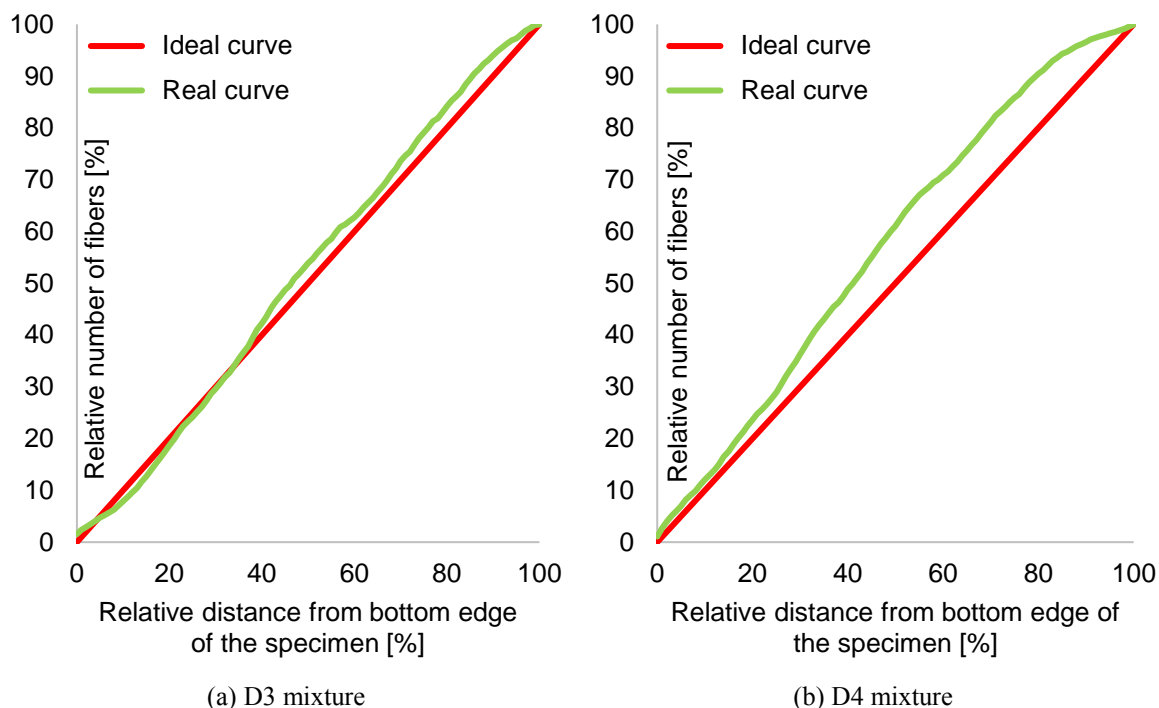


Fig. 10 Distribution of fibers in D3 and D4 mixtures

The worst distribution of fibers was determined in case of D4 series, where the average deviation between the real and ideal decomposition curve was  $\Delta = 7.7\%$ . This was probably caused by very fine nature of the mix. The biggest aggregate size was just 1 mm, a substantial part of the filler was replaced by cement. The fine mix was not able to support the fibers during the compaction process. Gravitational segregation of fibers occurred, the fibers settled to the bottom surface of the specimens.

D1 mixture also showed poor distribution of the fibers, having  $\Delta = 6.4\%$ . Assumed reason is that the grain size distribution curve of the aggregate was not smoothed out properly on the border between the two fractions used.

D2 and D3 mixtures reached excellent homogeneity. Values of  $\Delta$  calculated by ASEF were  $\Delta = 1.0\%$  in case of D2 and  $\Delta = 2.4\%$  for D3.

## 5.2 Homogeneity of SFRC for tunnel lining segments

ASEF is currently being tested as a supporting tool for control of dispersion of fibers in normal strength SFRC elements for bridges and tunnel lining segments in cooperation with one of the leading Central European construction companies (Vitek *et al.* 2016).

It is well known that the distribution of fibers in real structures is different from the distribution measured in standard cube specimens, mainly because the fiber orientation is influenced by the direction of concreting and by the surface area of the formwork (Resplendino *et al.* 2013). Therefore large scale specimens were used to control the dispersion of fibers in real scale.

In the case that will be described further, 400x500x1000 mm SFRC specimens were used to examine the distribution of fibers in SFRC mix designed for tunnel lining segments. The concrete \



Fig. 11 Sawing of large scale SFRC specimens

used for particular specimens contained various amounts ( $25 - 40 \text{ kg/m}^3$ ) of steel fibers 60 mm long, 0.75 mm in diameter, having the tensile strength of 1225 MPa. The specimens were concreted using the same technological equipment and casting method as for real elements. After hardening phase, the specimens were cut using circular saw (figure 11). Two sections (A, B) were evaluated for each of the five specimens (1 to 5). Section A was positioned 150 mm from the edge of the specimen, section B was located in the middle.

As the cross-sections of the samples were relatively large, it was not possible to take a photo suitable for the analysis in one step. Therefore each cross-section was photographed from several different angles and the final image was composed of several photos to reach the best possible contrast between the fibers and the matrix in all parts of the specimen (see figures 12 and 13).

A total of 10 specimens were evaluated (two 400 x 500 mm sections A and B from each of the five prismatic samples 1 to 5). The results are presented in table 2 and figures 14 and 15.

In most of the samples, slight settlement of the fibers was observed. There was relatively higher amount of fibers closer to the bottom edge of the specimen. The overall dispersion of the fibers was very close to the ideal one (see figure 15), reaching the average  $\Delta$  value of 4.2 %.

Data was exported from ASEF and further processed to calculate average and median distances between the fibers. Correlation coefficients between the number of fibers and distances between the fibers were calculated as -0.93 (number of fibers vs. average distance) and -0.86 (number of fibers vs. median distance). This very strong dependence indicates that the fibers were dispersed uniformly in the material without significant bundling of the fibers.

Except for specimen 1, almost the same amount of fibers was recorded in both sections A and B in each specimen, which again means that the mix was relatively homogeneous.

Deviation of fiber distribution curve from the ideal case was systematically higher in A section (at the edge of the specimen) than in B section (in the middle of the specimen). This was probably caused by inappropriate positioning of the surface vibrators attached to the formwork during production of the samples. Vibrators affected the outer part of the specimens more significantly than the inner part, leading to more pronounced settlement of the fibers.



Fig. 12 Source images of cross-section of specimen 4A. Selected areas are highlighted by yellow lines

Based on the results of the analysis in ASEF, it was decided that the concrete mix composition and concreting technique were designed correctly and that the material is suitable for the given purpose.

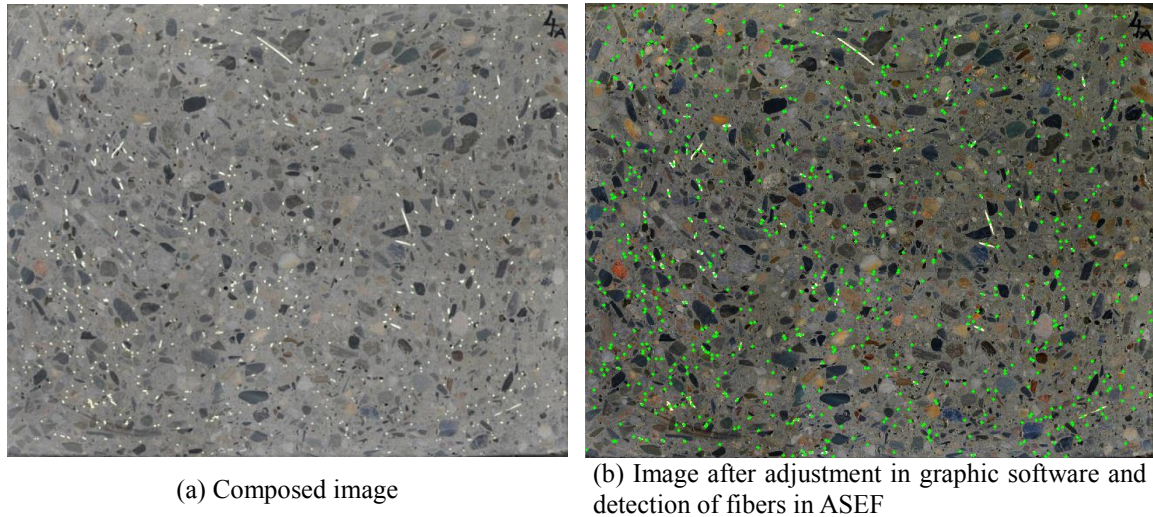


Fig. 13 Cross-section of specimen 4A

Table 2 Characteristics of particular specimens ( $f$  – amount of fibers per 1 m<sup>3</sup> of concrete;  $n$  – number of fibers;  $\Delta$  – see equation (7);  $\rho$  – see equation (8);  $l_{avg}$  = average distance between two fibers;  $l_{med}$  = median distance between two fibers.)

Specimen no.	$f$ [kg.m <sup>-3</sup> ]	$n$	$\Delta$ [%]	$P$ [%]	$l_{avg}$ [mm]	$l_{med}$ [mm]
1A	30	813	2.50	0.18	7.08	5.73
1B	30	1051	1.20	0.23	6.07	4.70
2A	40	1183	8.90	0.26	5.32	3.76
2B	40	1110	6.90	0.25	5.54	3.34
3A	32	921	1.20	0.20	6.02	4.51
3B	32	947	2.00	0.21	6.14	4.76
4A	25	685	4.80	0.15	7.26	5.70
4B	25	676	3.20	0.15	7.26	5.47
5A	35	942	8.50	0.21	6.62	4.89
5B	35	968	5.60	0.21	5.75	3.91

## 6. Conclusions

Computer aided digital image analysis method developed by the authors of this paper is a very interesting alternative to other existing methods of evaluation of distribution of steel fibers in hardened SFRC. The method is cheap, fast, simple and applicable in both laboratory and construction site. After cutting, the sample is illuminated (e.g. by halogen lamp from the construction site), the photo is taken (standard digital camera is sufficient), the image is adjusted in any available graphic software and analyzed in ASEF program. Clear, comprehensible and unbiased information about the distribution of fibers is obtained. Anyone possessing a digital camera and PC can use this method for quick and reliable analysis of SFRC homogeneity.

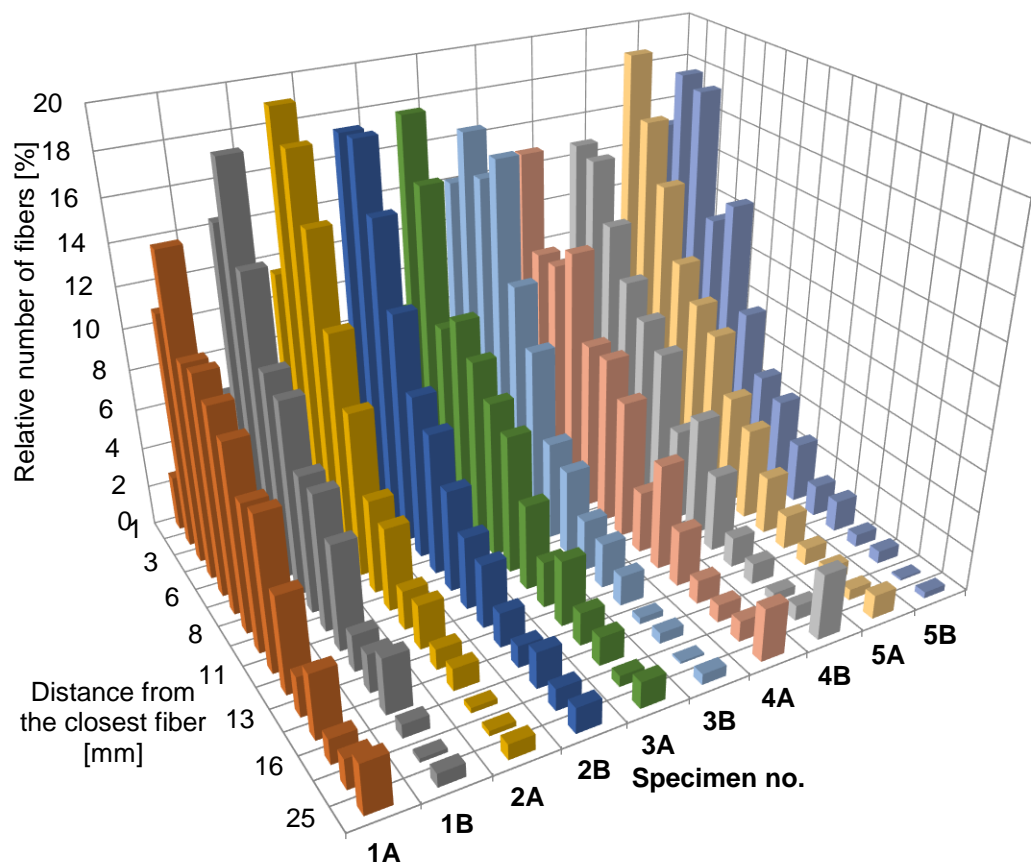


Fig. 14 Distances between the fibers in particular specimens

Thanks to the digital image analysis method, number of samples and working hours required for optimization of new concrete mixture can be decreased substantially. During construction, the approach can be exploited for periodic SFRC production quality control. The homogeneity is the key parameter of SFRC as the resistance of a SFRC member is given by the resistance of its weakest part. If the material produced is not homogeneous, the member may begin to fail at lower than design load, leading to financial loss connected with the repair.

Using the computer aided digital image analysis, it was proved that SFRC containing 120 kg of steel fibers per cubic meter of the mix can be produced with excellent homogeneity if the grain size distribution curve is amended accordingly.

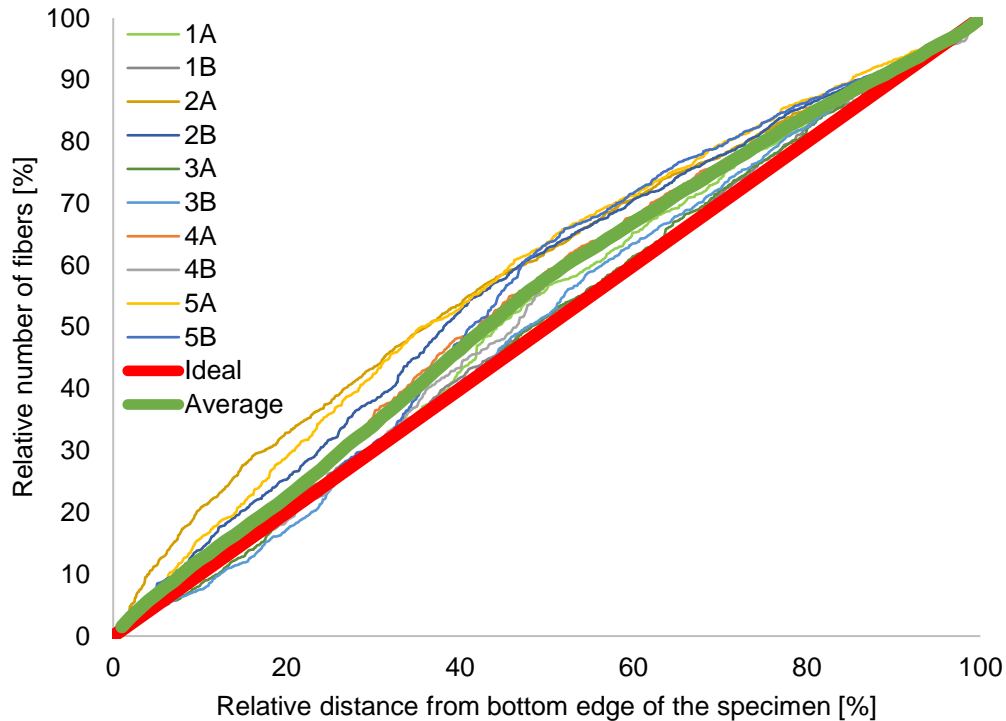


Fig. 15 Distribution of fibers in particular samples and average distribution

ASEF can be exploited for control of homogeneity of SFRC mixtures proposed for applications in all types of structures. An example of use of the program for analysis of large scale specimens made of SFRC mix designed for tunnel lining segments was presented in the paper. The analysis led to a conclusion that the quality of the mix is satisfactory for the given purpose.

### Acknowledgments

The preparation of this paper was enabled by the support of the Technology Agency of the Czech Republic (TAČR), project “Centre for Effective and Sustainable Transport Infrastructure” (no. TE01020168).

### References

- Abdelaziz, H.H., Meziane, M.A.A, Bousahla, A.A., Tounsi, A., Mahmoud, S.R. and Alwabli, A.S. (2017), “An efficient hyperbolic shear deformation theory for bending, buckling and free vibration of FGM sandwich plates with various boundary conditions”, *Steel Compos. Struct.*, **25**(6), 693-704. <https://doi.org/10.12989/scs.2017.25.6.693>.
- Abualnour, M., Houari, M.S.A., Tounsi, A., Adda Bedia, E.A. and Mahmoud, S.R. (2018), “A novel quasi-3D trigonometric plate theory for free vibration analysis of advanced composite plates”, *Compos. Struct.*, **184**, 688-697. <https://doi.org/10.1016/j.compstruct.2017.10.047>,
- Ahmed, A. (2014), “Post buckling analysis of sandwich beams with functionally graded faces using a

- consistent higher order theory”, *Int. J. Civil, Struct. Envir.*, **4**(2), 59-64.
- Ait Atmane, H., Tounsi, A., Bernard, F. and Mahmoud, S.R. (2015), “A computational shear displacement model for vibrational analysis of functionally graded beams with porosities”, *Steel Compos. Struct.*, **19**(2), 369-384. <https://doi.org/10.12989/scs.2015.19.2.369>.
- Ait Atmane, H., Tounsi, A. and Bernard, F. (2017), “Effect of thickness stretching and porosity on mechanical response of a functionally graded beams resting on elastic foundations”, *Int. J. Mech. Mater. Des.*, **13**(1), 71-84. <https://doi.org/10.1007/s10999-015-9318-x>.
- Ait Yahia, S., Ait Atmane, H., Houari, M.S.A. and Tounsi, A. (2015), “Wave propagation in functionally graded plates with porosities using various higher-order shear deformation plate theories”, *Struct. Eng. Mech.*, **53**(6), 1143-1165. <http://dx.doi.org/10.12989/sem.2015.53.6.1143>.
- Akavci, S.S. (2016), “Mechanical behavior of functionally graded sandwich plates on elastic foundation”, *Composites Part B*, **96**, 136-152. <https://doi.org/10.1016/j.compositesb.2016.04.035>.
- Akbas, S.D. (2016), “Forced vibration analysis of viscoelastic nanobeams embedded in an elastic medium”, *Smart Struct. Syst.*, **18**(6), 1125-1143. <http://dx.doi.org/10.12989/sss.2016.18.6.1125>.
- Aldousari, S.M. (2017), “Bending analysis of different material distributions of functionally graded beam”, *Appl. Phys. A*, **123**, 296. <https://doi.org/10.1007/s00339-017-0854-0>.
- Attia, A., Bousahla, A.A., Tounsi, A., Mahmoud, S.R. and Alwabri, A.S. (2018), “A refined four variable plate theory for thermoelastic analysis of FGM plates resting on variable elastic foundations”, *Struct. Eng. Mech.*, **65**(4), 453-464. <https://doi.org/10.12989/sem.2018.65.4.453>.
- Avcar, M. (2015), “Effects of rotary inertia shear deformation and non-homogeneity on frequencies of beam”, *Struct Eng Mech*, **55**, 871-884. <http://dx.doi.org/10.12989/sem.2015.55.4.871>.
- Avcar, M. (2016), “Effects of material non-homogeneity and two-parameter elastic foundation on fundamental frequency parameters of Timoshenko beams”, *Acta Physica Polonica A*, **130**(1), 375-378. <https://doi.org/10.12693/APhysPolA.130.375>.
- Avcar, M., & Mohammed, W.K.M. (2018), “Free vibration of functionally graded beams resting on Winkler-Pasternak foundation”, *Arabian J. Geosci.*, **11**(10), 232. <https://doi.org/10.1007/s12517-018-3579-2>.
- Avcar, M. (2019), “Free vibration of imperfect sigmoid and power law functionally graded beams”, *Steel Compos. Struct.*, **30**(6), 603-615.
- Bakhadda, B., Bachir Bouiadjra, M., Bourada, F., Bousahla, A.A., Tounsi, A. and Mahmoud, S.R. (2018), “Dynamic and bending analysis of carbon nanotube-reinforced composite plates with elastic foundation”, *Wind Struct.*, **27**(5), 311-324. <https://doi.org/10.12989/was.2018.27.5.311>.
- Becheri, T., Amara, K., Bouazza, M. and Benseddiq, N. (2016), “Buckling of symmetrically laminated plates using nth-order shear deformation theory with curvature effects”, *Steel Compos. Struct.*, **21**(6), 1347-1368.
- Behravan Rad, A. (2015), “Thermo-elastic analysis of functionally graded circular plates resting on a gradient hybrid foundation”, *Appl. Math. Comput.*, **256**, 276-298. <https://doi.org/10.1016/j.amc.2015.01.026>.
- Belabed, Z., Houari, M.S.A., Tounsi, A., Mahmoud, S.R. and Anwar Bég, O. (2014), “An efficient and simple higher order shear and normal deformation theory for functionally graded material (FGM) plates”, *Compos. Part B*, **60**, 274-283. <https://doi.org/10.1016/j.compositesb.2013.12.057>.
- Belabed, Z., Bousahla, A.A., Houari, M.S.A., Tounsi, A. and Mahmoud, S.R. (2018), “A new 3-unknown hyperbolic shear deformation theory for vibration of functionally graded sandwich plate”, *Earthq. Struct.*, **14**(2), 103-115. <http://dx.doi.org/10.12989/eas.2018.14.2.103>.
- Beldjelili, Y., Tounsi, A. and Mahmoud, S.R. (2016), “Hygro-thermo-mechanical bending of S-FGM plates resting on variable elastic foundations using a four-variable trigonometric plate theory”, *Smart Struct. Syst.*, **18**(4), 755-786. <http://dx.doi.org/10.12989/sss.2016.18.4.755>.
- Bellifa, H., Benrahou, K.H., Hadji, L., Houari, M.S.A. and Tounsi, A. (2016), “Bending and free vibration analysis of functionally graded plates using a simple shear deformation theory and the concept of the neutral surface position”, *J. Braz. Soc. Mech. Sci. Eng.*, **38**(1), 265-275. <https://doi.org/10.1007/s40430-015-0354-0>.
- Bellifa, H., Bakora, A., Tounsi, A., Bousahla, A.A. and Mahmoud, S.R. (2017), “An efficient and simple

- four variable refined plate theory for buckling analysis of functionally graded plates”, *Steel Compos. Struct.*, **25**(3), 257-270. <http://dx.doi.org/10.12989/scs.2017.25.3.257>.
- Benadouda, M., Ait Atmane, Hassen., Tounsi, A., Bernard, Fabrice. and Mahmoud, S.R. (2017), “An efficient shear deformation theory for wave propagation in functionally graded material beams with porosities”, *Earthq. Struct.*, **13**(3), 255-265. <http://dx.doi.org/10.12989/eas.2017.13.3.255>.
- Benahmed, A., Houari, M.S.A., Benyoucef, S., Belakhdar, K. and Tounsi, A. (2017), “A novel quasi-3D hyperbolic shear deformation theory for functionally graded thick rectangular plates on elastic foundation”, *Geomech. Eng.*, **12**(1), 9-34. <http://dx.doi.org/10.12989/gae.2017.12.1.009>.
- Benbakhti, A., Bachir Bouiadjra, M., Retiel, N. and Tounsi, A. (2016), “A new five unknown quasi-3D type HSDT for thermomechanical bending analysis of FGM sandwich plates”, *Steel Compos. Struct.*, **22**(5), 975-999. <http://dx.doi.org/10.12989/scs.2016.22.5.975>.
- Benchohra, M., Driz, H., Bakora, A., Tounsi, A., Adda Bedia, E.A. and Mahmoud, S.R. (2018), “A new quasi-3D sinusoidal shear deformation theory for functionally graded plates”, *Struct. Eng. Mech.*, **65**(1), 19-31. <http://dx.doi.org/10.12989/sem.2018.65.1.019>.
- Bennai, R., Ait Atmane, H. and Tounsi, A. (2015), “A new higher-order shear and normal deformation theory for functionally graded sandwich beams”, *Steel Compos. Struct.*, **19**(3), 521-546. <http://dx.doi.org/10.12989/scs.2015.19.3.521>.
- Bennoun, M., Houari, M.S.A. and Tounsi, A. (2016), “A novel five variable refined plate theory for vibration analysis of functionally graded sandwich plates”, *Mech. Adv. Mater. Struct.*, **23**(4), 423-431. <https://doi.org/10.1080/15376494.2014.984088>.
- Benzair, A., Tounsi, A., Besseghier, A., Heireche, H., Moulay, N. and Boumia, L. (2008), “The thermal effect on vibration of single-walled carbon nanotubes using nonlocal Timoshenko beam theory”, *J. Phys. D: Appl. Phys.*, **41**, 225404.
- Berrabah, H.M., Tounsi, A., Semmah, A. and Adda Bedia, E.A. (2013), “Comparison of various refined nonlocal beam theories for bending, vibration and buckling analysis of nanobeams”, *Struct. Eng. Mech.*, **48**(3), 351-365. <http://dx.doi.org/10.12989/sem.2013.48.3.351>.
- Bhangale, R. K. and Ganesan, N.(2006), “Thermoelastic buckling and vibration behavior of a functionally graded sandwich beam with constrained viscoelastic core”, *J. Sound Vib.*, **295**(12), 294-316. <https://doi.org/10.1016/j.jsv.2006.01.026>.
- Bouafia, K., Kaci, A., Houari, M.S.A., Benzair, A. and Tounsi, A. (2017), “A nonlocal quasi-3D theory for bending and free flexural vibration behaviors of functionally graded nanobeams”, *Smart Struct. Syst.*, **19**(2), 115-126. <http://dx.doi.org/10.12989/sss.2017.19.2.115>.
- Bouazza, M., Lairedj, A., Benseddiq, N. and Khalki, S. (2016), “A refined hyperbolic shear deformation theory for thermal buckling analysis of cross-ply laminated plates”, *Mech Res Commun*, **73**, 117-126. <https://doi.org/10.1016/j.mechrescom.2016.02.015>.
- Bouazza, M., Zenkour, A.M. and Benseddiq, N. (2018), “Closed-form solutions for thermal buckling analyses of advanced nanoplates according to a hyperbolic four-variable refined theory with small-scale effects”, *Acta Mech*, **229**(5), 2251-2265. <https://doi.org/10.1007/s00707-017-2097-8>.
- Bouderba, B., Houari, M.S.A. and Tounsi, A. and Mahmoud, S.R. (2016), “Thermal stability of functionally graded sandwich plates using a simple shear deformation theory”, *Struct. Eng. Mech., Int. J.*, **58**(3), 397-422. <http://dx.doi.org/10.12989/sem.2016.58.3.397>.
- Bourada, F., Bousahla, A.A., Bourada, M., Azzaz, A., Zinata, A. and Tounsi, A. (2019), “Dynamic investigation of porous functionally graded beam using a sinusoidal shear deformation theory”, *Wind Struct.*, **28**(1), 19-30. <http://dx.doi.org/10.12989/was.2019.28.1.019>.
- Bourada, F., Amara, K., Bousahla, A.A., Tounsi, A. and Mahmoud, S.R. (2018), “A novel refined plate theory for stability analysis of hybrid and symmetric S-FGM plates”, *Struct. Eng. Mech.*, **68**(6), 661-675. <http://dx.doi.org/10.12989/sem.2018.68.6.661>.
- Bourada, M., Kaci, A., Houari, M.S.A. and Tounsi, A. (2015), “A new simple shear and normal deformations theory for functionally graded beams”, *Steel Compos. Struct. Int. J.*, **18**(2), 409-423. <http://dx.doi.org/10.12989/scs.2015.18.2.409>.
- Bourada, M., Tounsi, A., Houari, M.S.A. and Adda Bedia, E.A. (2012), “A new four-variable refined plate

- theory for thermal buckling analysis of functionally graded sandwich plates”, *J. Sandwich Structures Materials*, **14**, 5-33. <https://doi.org/10.1177/1099636211426386>.
- Bui, T.Q., Khosravifard, A., Zhang, C., Hematiyan, M.R. and Golub, M.V. (2013), “Dynamic analysis of sandwich beams with functionally graded core using a truly meshfree radial point interpolation method”, *Eng. Struct.*, **47**, 90-104. <https://doi.org/10.1016/j.engstruct.2012.03.041>.
- Carrera, E., Brischetto, S., Cinefra, M. and Soave, M. (2011), “Effects of thickness stretching in functionally graded plates and shells”, *Compos. Part B Eng.*, **42**(2), 123-133. <https://doi.org/10.1016/j.compositesb.2010.10.005>.
- Chen, C.S., Hsu, C.Y. and Tzou, G.J. (2009), “Vibration and stability of functionally graded plates based on a higher-order deformation theory”, *J. Reinf. Plast. Compos.*, **28**(10), 1215-1234. <https://doi.org/10.1177/0731684408088884>
- Dash, S., Mehar, K., Sharma, N., Mahapatra, T.R. and Panda, S.K. (2018), “Modal analysis of FG sandwich doubly curved shell structure”, *Struct. Eng. Mech.*, **68**(6), 721-733. <https://doi.org/10.12989/sem.2018.68.6.721>.
- Dash, S., Mehar, K., Sharma, N., Mahapatra, T.R. and Panda, S.K. (2019), “Finite element solution of stress and flexural strength of functionally graded doubly curved sandwich shell panel”, *Earthq. Struct.*, **16**(1), 55-67. <http://dx.doi.org/10.12989/eas.2019.16.1.055>.
- Dellal, F. and Erdogan, F. (1983), “The crack problem for a non-homogeneous plane”, *ASME J. Applied Mechanics*, **50**, 609. <https://doi.org/10.1115/1.3167098>.
- Draiche, K., Tounsi, A. and Mahmoud, S.R. (2016), “A refined theory with stretching effect for the flexure analysis of laminated composite plates”, *Geomech. Eng.*, **11**(5), 671-690. <http://dx.doi.org/10.12989/gae.2016.11.5.671>.
- Faleh, N.M., Ahmed, R.A. and Fenjan, R.M. (2018), “On vibrations of porous FG nanoshells”, *J. Eng. Sci.*, **133**, 1-14. <https://doi.org/10.1115/1.3167098>
- Hamidi, A., Houari, M.S.A., Mahmoud, S.R. and Tounsi, A. (2015), “A sinusoidal plate theory with 5-unknowns and stretching effect for thermomechanical bending of functionally graded sandwich plates”, *Steel Compos. Struct.*, **18**(1), 235-253. <https://doi.org/10.12989/scs.2015.18.1.235>.
- Hebali, H., Tounsi, A., Houari, M.S.A., Bessaim, A. and Adda Bedia, E.A. (2014), “A new quasi-3D hyperbolic shear deformation theory for the static and free vibration analysis of functionally graded plates”, *ASCE J. Eng. Mech.*, **140**(2), 374-383.
- Houari, M.S.A., Tounsi, A., Bessaim, A. and Mahmoud, S.R. (2016), “A new simple three-unknown sinusoidal shear deformation theory for functionally graded plates”, *Steel Compos. Struct.*, **22**(2), 257-276. <http://dx.doi.org/10.12989/scs.2016.22.2.257>.
- Karami, B., Janghorban, M., Shahsavari, D. and Tounsi, A. (2018), “A size-dependent quasi-3D model for wave dispersion analysis of FG nanoplates”, *Steel Compos. Struct.*, **28**(1), 99-110. <http://dx.doi.org/10.12989/scs.2018.28.1.099>.
- Kar, V.R. and Panda, S.K. (2015), “Nonlinear flexural vibration of shear deformable functionally graded spherical shell panel”, *Steel Compos. Struct., Int. J.*, **18**(3), 693-709. <http://dx.doi.org/10.12989/scs.2015.18.3.693>.
- Kar, V.R. and Panda, S.K. (2016), “Post-buckling behaviour of shear deformable functionally graded curved shell panel under edge compression”, *J. Mech. Sci.*, **115**, 318-324. <https://doi.org/10.1016/j.ijmecsci.2016.07.014>,
- Kar, V.R. and Panda, S.K., Mahapatra, T.R. (2016), “Thermal buckling behaviour of shear deformable functionally graded single/doubly curved shell panel with TD and TID properties”, *Adv. Mater. Res.*, **5**(4), 205-221. <http://dx.doi.org/10.12989/amr.2016.5.4.205>.
- Kar, V.R., Mahapatra, T.R. and Panda, S.K. (2017), “Effect of different temperature load on thermal postbuckling behaviour of functionally graded shallow curved shell panels”, *Compos. Struct.*, **160**, 1236-1247. <https://doi.org/10.1016/j.compstruct.2016.10.125>.
- Kar, V.R. and Panda, S.K. (2017), “Postbuckling analysis of shear deformable FG shallow spherical shell panel under nonuniform thermal environment”, *J. Thermal Stresses*, **40**(1), 25-39. <https://doi.org/10.1080/01495739.2016.1207118>.

- Katariya, P.V. and Panda, S.K. (2016), "Thermal buckling and vibration analysis of laminated composite curved shell panel", *Aircraft Eng. Aerosp. Technol.*, **88**(1), 97-107.
- Katariya, P.V., Panda, S.K., Hirwani, C.K., Mehar, K. and Thakare, O. (2017a), "Enhancement of thermal buckling strength of laminated sandwich composite panel structure embedded with shape memory alloy fibre", *Smart Struct. Syst.*, **20**(5), 595-605. <http://dx.doi.org/10.12989/sss.2017.20.5.595>.
- Katariya, P.V., Panda, S.K., Mahapatra, T.R. (2017b), "Nonlinear thermal buckling behaviour of laminated composite panel structure including the stretching effect and higher-order finite element", *Adv. Mater. Res.*, **6**(4), 349-361. <http://dx.doi.org/10.12989/amr.2017.6.4.349>.
- Katariya, P.V., Das, A. and Panda, S.K. (2018), "Buckling analysis of SMA bonded sandwich structure – using FEM", *IOP Conference Series: Materials Science and Engineering*, **338**(1), 012035.
- Khiloun, M., Bousahla, A.A., Kaci, A., Bessaim, A., Tounsi, A. and Mahmoud, S.R. (2019), "Analytical modeling of bending and vibration of thick advanced composite plates using a four-variable quasi 3D HSDT", *Eng. with Comput.* <https://doi.org/10.1007/s00366-019-00732-1>.
- Kolahchi, R., Bidgoli, A.M.M. and Heydari, M.M. (2015), "Size-dependent bending analysis of FGM sinusoidal plates resting on orthotropic elastic medium", *Struct. Eng. Mech.*, **55**(5), 1001-1014. <http://dx.doi.org/10.12989/sem.2015.55.5.1001>.
- Larbi Chaht, F., Kaci, A., Houari, M.S.A., Tounsi, A., Anwar Bég, O. and Mahmoud, S.R. (2015), "Bending and buckling analyses of functionally graded material (FGM) size-dependent nanoscale beams including the thickness stretching effect", *Steel Compos. Struct., Int. J.*, **18**(2), 425-442. <http://dx.doi.org/10.12989/scs.2015.18.2.425>
- Mahmoud, S.R. and Tounsi, A. (2017), "A new shear deformation plate theory with stretching effect for buckling analysis of functionally graded sandwich plates", *Steel Compos. Struct.*, **24**(5), 569-578. <http://dx.doi.org/10.12989/scs.2017.24.5.569>.
- Matsunaga, H. (2008), "Free vibration and stability of functionally graded plates according to a 2-D higher-order deformation theory", *Compos. Struct.*, **82**(4), 499-512. <https://doi.org/10.1016/j.compstruct.2007.01.030>.
- Mehar, K., Panda, S.K. and Mahapatra, T.R. (2017), "Thermoelastic nonlinear frequency analysis of CNT reinforced functionally graded sandwich structure", *European J. Mech.-A/Solids*, **65**, 384-396. <https://doi.org/10.1016/j.euromechsol.2017.05.005>.
- Mehar, K. and Panda, S.K. (2018), "Thermal free vibration behavior of FG-CNT reinforced sandwich curved panel using finite element method", *Polymer Composites*, **39**(8), 2751-2764. <https://doi.org/10.1002/pc.24266>.
- Mehar, K., Panda, S.K., Devarajan, Y. and Choubey, G. (2019), "Numerical buckling analysis of graded CNT-reinforced composite sandwich shell structure under thermal loading", *Compos. Struct.*, **216**, 406-414. <https://doi.org/10.1016/j.compstruct.2019.03.002>.
- Mouli, B.C., Ramji, K., Kar, V.R., Panda, S.K., Lalepalli, A.K. and Pandey, H.K. (2018), "Numerical study of temperature dependent eigenfrequency responses of tilted functionally graded shallow shell structures", *Struct. Eng. Mech.*, **68**(5), 527-536. <http://dx.doi.org/10.12989/sem.2018.68.5.527>.
- Neves, A.M.A., Ferreira, A.J.M., Carrera E., Cinefra M., Jorge R.M.N. and Soares C.M.M. (2012), "Buckling analysis of sandwich plates with functionally graded skins using a new quasi-3D hyperbolic sine shear deformation theory and collocation with radial basis functions", *ZAMM*, **92**(9), 749-766. <https://doi.org/10.1002/zamm.201100186>.
- Panda, S.K. and Katariya, P.V. (2015), "Stability and free vibration behaviour of laminated composite panels under thermo-mechanical loading", *J. Appl. Comput. Math.*, **1**(3), 475-490. <https://doi.org/10.1007/s40819-015-0035-9>.
- Reddy, J.N. (2000), "Analysis of functionally graded plates", *Int. J. Numer. Meth. Eng.*, **47**(1-3), 663-684.
- Reddy, J.N. (2011), "A general nonlinear third-order theory of functionally graded plates", *Int. J. Aerosp. Lightw. Struct.*, **1**(1), 1-21. <http://dx.doi.org/10.3850/S201042861100002X>.
- Sekkal, M., Fahsi, B., Tounsi, A. and Mahmoud, S.R. (2017), "A new quasi-3D HSDT for buckling and vibration of FG plate", *Struct. Eng. Mech.*, **64**(6), 737-749. <http://dx.doi.org/10.12989/2017.64.6.737>.
- Semmah, A, Tounsi, A., Zidour, M., Heireche, H. and Naceri, M. (2014), "Effect of chirality on critical

- buckling temperature of a zigzag single-walled carbon nanotubes using nonlocal continuum theory”, *Full., Nanotub. Carbon Nanostr.*, **23**, 518-522. <https://doi.org/10.1080/1536383X.2012.749457>.
- Shahsavari, D., Shahsavari, M., Li, L. and Karami, B. (2018), “A novel quasi-3D hyperbolic theory for free vibration of FG plates with porosities resting on Winkler/Pasternak/Kerr foundation”, *Aerosp. Sci. Technol.*, **72**, 134-149. <https://doi.org/10.1016/j.ast.2017.11.004>.
- Sharma, N., Mahapatra, T.R., Panda, S.K. and Mehar, K. (2018), “Evaluation of vibroacoustic responses of laminated composite sandwich structure using higher-order finite-boundary element model”, *Steel Compos. Struct.*, **28**(5), 629-639. <http://dx.doi.org/10.12989/scs.2018.28.5.629>.
- Sobhy, M. (2013), “Buckling and free vibration of exponentially graded sandwich plates resting on elastic foundations under various boundary conditions”, *Compos. Struct.*, **99**, 76-87. <https://doi.org/10.1016/j.compstruct.2012.11.018>.
- Swaminathan, K. and Naveenkumar, D.T. (2014), “Higher order refined computational models for the stability analysis of FGM plates: Analytical solutions”, *Eur. J. Mech. A/Solid.*, **47**, 349-361. <https://doi.org/10.1016/j.euromechsol.2014.06.003>.
- Xiang, S., Jin, Y.X., Bi, Z.Y., Jiang, S.X. and Yang, M.S. (2011), “A n-order shear deformation theory for free vibration of functionally graded and composite sandwich plates”, *Compos. Struct.*, **93**(11), 2826-2832. <https://doi.org/10.1016/j.compstruct.2011.05.022>.
- Zaoui, F.Z., Ouinas, D. and Tounsi, A. (2019), “New 2D and quasi-3D shear deformation theories for free vibration of functionally graded plates on elastic foundations”, *Compos. Part B*, **159**, 231-247. <https://doi.org/10.1016/j.compositesb.2018.09.051>.
- Zenkour, M. (2005), “A comprehensive analysis of functionally graded sandwich plates: Part2—Buckling and free vibration”, *Int. J. of Solids Struct.*, **42**, 5243-5258. <https://doi.org/10.1016/j.ijsolstr.2005.02.016>.
- Zenkour, A.M. and Sobhy, M. (2010), “Thermal buckling of various types of FGM sandwich plates”, *Compos. Struct.*, **93**, 93-102. <https://doi.org/10.1016/j.compstruct.2010.06.012>.
- Zenkour, A.M., Allam, M.N.M. and Sobhy, M. (2010), “Bending analysis of FG visco-elastic sandwich beams with elastic cores resting on Pasternak’s elastic foundations”, *Acta Mech.*, **212**, 233-252. <https://doi.org/10.1007/s00707-009-0252-6>.